Nanoscale

PAPER

View Article Online
View Journal | View Issue

Cite this: *Nanoscale*, 2014, **6**, 9215

Stem-loop DNA-assisted silicon nanowires-based biochemical sensors with ultra-high sensitivity, specificity, and multiplexing capability†

Juan Xie, Xiangxu Jiang, Yiling Zhong, Yimei Lu, Siyi Wang, Xinpan Wei, Yuanyuan Su and Yao He*

Received 27th February 2014
Accepted 4th June 2014

DOI: 10.1039/c4nr01097c

www.rsc.org/nanoscale

A class of stem-loop DNA-assisted silicon nanowires (SiNWs)-based fluorescent biosensor is presented in this report. Significantly, the sensor enables rapid and sensitive detection of DNA targets with a concentration as low as 1 pM. Moreover, the large planar surface of SiNWs facilitates simultaneous assembly with different DNA strands, which is favorable for multiplexed DNA detection. On the other hand, the SiNWs-based sensor is highly efficacious for detecting heavy metal ions. Mercury ions (Hg^{2+}) of low concentrations (*e.g.*, 5 pM) are readily identified from its mixture with over 10 kinds of interfering metal ions, even in real water samples. Given that SiNWs can be fabricated in a facile, reproducible and low-cost manner, this kind of SiNWs-based high-performance sensor is expected to be a practical analytical tool for a variety of biological and environment-protection applications.

Introduction

There is an ever increasing requirement for developing sensitive, selective, and cost-effective biochemical sensing strategies in myriad chemical and biological applications. This explains the extensive attention given to well-known methods such as electrical, optical, and magnetic detection methods.[1–3] Among them, optical techniques are highly promising because of their high specificity and sensitivity. As is well known, nanomaterials of unique optical properties have shown highly attractive opportunities for myriad chemical and biological analyses in the past two decades.[4–6] Typically, semiconductor fluorescent quantum dots (QDs), known as highly fluorescent nanoprobes, have been widely used for bioimaging and biosensing applications due to their strong luminescence, robust photostability, and size-tunable emission color.[7–9] Silver and gold nanoparticles (NPs), serving as surface enhanced Raman scattering (SERS) substrates, have been employed for ultra-high sensitive sensing applications.[10–15] Recently, various kinds of nanomaterials (*e.g.*, gold nanoparticles (AuNPs), graphene, and carbon nanotubes) have been utilized as novel fluorescent quenchers for constructing nano-molecular beacons (nanoMBs), enabling sensitive and multiplexed DNA detection.[16–22]

Silicon nanomaterials have attracted extensive attention due to a number of traits.[23–28] Among them, silicon nanowires (SiNWs) have been widely explored for a variety of electronic and biological applications.[29–40] SiNWs-based bioapplications are of particular interest, including our recent success in designing SiNWs-based nanoprobes and nanoagents for tumor detection and treatment.[38–40] In particular, photostable SiNWs-based nanoprobes have been employed for bioimaging application in a long-term manner.[38] SiNWs-based near-infrared (NIR) hyperthermia agents, featuring significant photo-thermal effects, can efficiently kill malignant tumor cells.[39] Very recently, taking advantage of large surface-to-volume ratio and porous structure, we further developed a class of SiNWs-based drug nanocarriers capable of cancer treatment *in vitro* and *in vivo*.[40]

By utilizing high quenching efficiency (QE > 90%), large surface-to-volume ratio, and facile surface tailorability of SiNWs, we herein employ stem-loop DNA and SiNWs for fabricating a novel type of SiNWs-based fluorescent sensors featuring high sensitivity, specificity, and multiplexing capabilities. In principle, fluorescent signals can effectively switch between "on" and "off" states by adjusting distance between the SiNWs and fluorescein tagged with DNA. As a result, biological and chemical species of low concentrations (*e.g.*, DNA and Hg^{2+} at ~pM levels) can be readily detected, based on disruption or formation of stem-loop configuration in the presence of targets. In addition to high sensitivity, the resultant SiNWs-based sensors feature multiplexing capabilities because of the huge surface area and high surface-to-volume ratio of SiNWs, facilitating simultaneous detection of multiple DNA strands. Moreover, we further demonstrate that the prepared sensors are suitable for detection of mercury ions (Hg^{2+}) of low concentrations (5 pM) in a real system.

Institute of Functional Nano & Soft Materials (FUNSOM), Collaborative Innovation Center of Suzhou Nano Science and Technology, Soochow University, Suzhou, Jiangsu 215123, China. E-mail: yaohe@suda.edu.cn; Fax: +86-512-65880946

† Electronic supplementary information (ESI) available. See DOI: 10.1039/c4nr01097c

Results and discussion

As schematically illustrated in Fig. 1, free SiNWs synthesized through an established HF-assisted etching (HAE) strategy[41–44] are first modified with glutaraldehyde (GA) on their surface. The steps are as follows: the SiNW surface is treated with O_2 plasma to confer hydroxyl groups (Step 1), and then further conjugated with APTES in the second step (Step 2). Thereafter, GA molecules are reacted with APTES molecules (Step 3), producing GA-modified SiNW that is ready for assembly with DNA that is tagged with amino group and organic dye molecule (*e.g.*, Cy5) at 3 and 5, respectively, by the Schiff reaction.[45,46] Notably, the resultant stem-loop DNA-functionalized SiNW yields feeble fluorescence since Cy5 molecules are close to SiNW surface (SiNWs feature high fluorescence quenching efficiency over 90%, please see detailed data and discussion in Fig. 3). In contrast, hybridization between capture DNA and target DNA would lead to disruption of the stem-loop configuration, resulting in effective separation of SiNW surface and dye molecules. Therefore, fluorescence is distinctly enhanced, capable of detection of target DNA based on observing the fluorescence enhancement (so-called "signal-on" procedure, Step 4). On the other hand, for Hg^{2+} detection, the GA-modified SiNW is first assembled with Cy5-tagged thymine-rich DNA strands (*i.e.*, T-rich mercury-specific oligonucleotide (MSO), Step 4′), yielding strong fluorescence owing to relatively long distance between Cy5 molecules and SiNW surface (*i.e.*, signal-on state). After adding Hg^{2+} ions, the two ends of DNA become close to each other through thymine–Hg–thymine base pair formation, leading to distinct SiNW-induced fluorescence quenching (Step 5′). As a result, Hg^{2+} ions can be sensitively and specifically detected *via* quantitatively analyzing decrease in fluorescence intensities.

A well-studied HAE approach was utilized for production of free SiNW (diameter: ~100 nm, length: 4 μm) arrays (Fig. 2a and b).[41–44] Fig. 2c and d presents typical transmission electronic microscopy (TEM) and high-resolution TEM images of a single GA-modified SiNW, showing clear crystal planes of the SiNW with [110] growth direction. Moreover, dark-field scanning TEM (STEM) images confirm that the modified SiNW contains C, O, or Si element, as indicated by red, brown, or yellow color in Fig. 2e, respectively. FTIR is also employed for investigating alteration of chemical bonding induced by surface modification. As shown in Fig. 2f, significant absorption peaks located in 1000–3500 cm^{-1} are observed for both pure SiNWs and modified SiNWs, among which the 3440 cm^{-1} peak is attributed to O–H stretching vibration.[47,48] Compared to the peak of the pure SiNWs (black line), the sharper and stronger 1060 cm^{-1} peak (vibration stretch of Si–O bonding) of the modified SiNWs indicates the formation of more Si–O bonds,[43,49] which are produced by O_2 plasma-treatment (red line). For the SiNWs conjugated with APTES (blue line), the strong absorbance in the ranges of 1016–1130, 1580, and 2930 cm^{-1} are observed, which is attributed to the Si–O–Si, N–H, and C–H bond, respectively, confirming that the resultant SiNWs have a large amount of amido groups.[48,50,51] In case of the GA-modified SiNWs, the spectrum (green line) shows a distinct peak located at 1720 cm^{-1} (C═O stretching vibration) due to their surface-covered aldehyde groups.[43,52]

Quenching efficiency (QE) is calculated based on an established equation:[16,20,44]

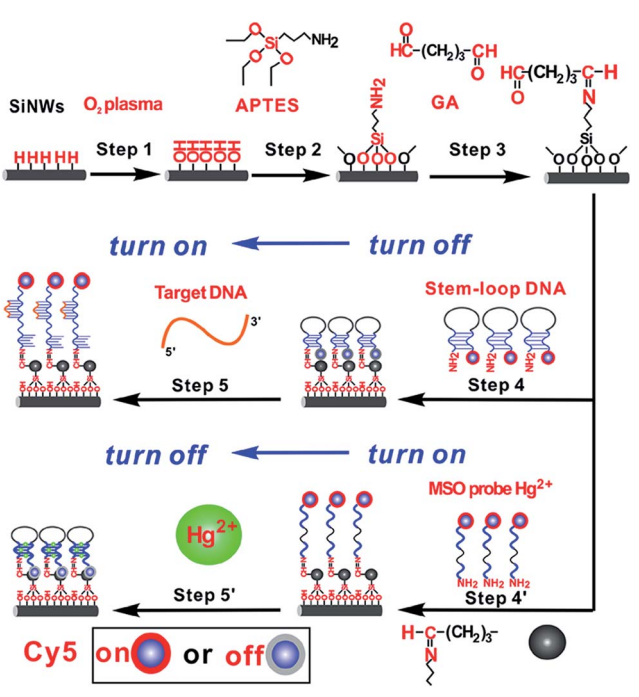

Fig. 1 Schematic diagram of construction of SiNWs-based fluorescent sensor for DNA and Hg^{2+} detection.

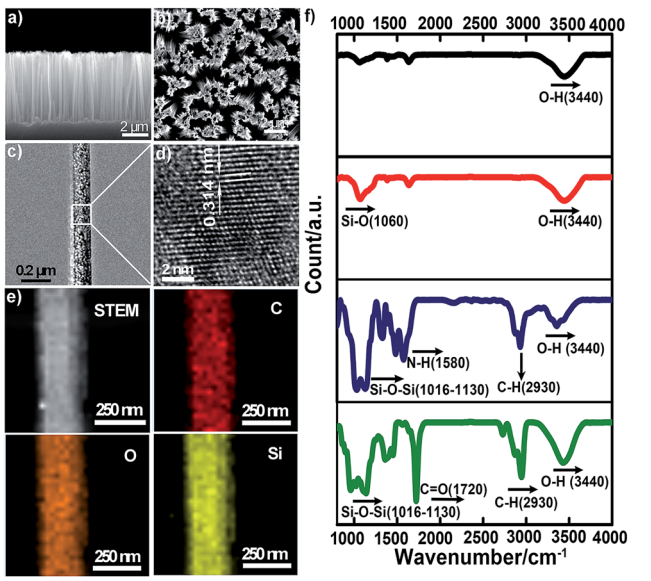

Fig. 2 Cross-section (a) and top view (b) SEM images of the modified SiNW arrays. TEM (c) and HRTEM (d) overview images of the GA-modified SiNW. (e) STEM and corresponding energy-dispersive X-ray spectroscopy (EDX) element mapping of the GA-modified SiNW. (f) FTIR spectra of free SiNWs (black line), the O_2 plasma-treated SiNWs (red line), the APTES-conjugated SiNWs (blue line), and the GA-modified SiNWs (green line).

$$QE = (I_{dye} - I_{SiNWs})/(I_{dye}) \quad (1)$$

where I_{dye} and I_{SiNWs} stand for fluorescent intensities of organic dyes and SiNWs, which are determined according to fluorescent spectra of free SiNWs-treated organics. As shown in Fig. 3, SiNWs lead to severe fluorescence quenching towards FAM, Cy5, and ROX, indicating that the SiNWs possess high QE values (>90%) for the three types of organic dyes. This is attributed to high-efficacy energy transfer from SiNWs to organic dyes, consistent with previous reports introducing AuNPs or CNTs-based quenchers of similarly high QE values of ~90%.[16,18,20] Moreover, the nanowire-based structures may facilitate enhancement of charge transportation, which is considered as another positive factor for the observed high QE value of SiNWs.

To verify that GA molecules are modified on the SiNW surface, stem-loop configuration transformation-induced change of fluorescent intensities are visually compared in parallel experiments by Maestro *in vivo* imaging system. As shown in Fig. 4a and b, the red signal of Cy5 is feeble without target DNA, which is due to SiNW-induced fluorescence quenching. Once hybridizing with a complementary target sequence, fluorescent intensity of Cy5 is largely recovered since the loop structures are destroyed, yielding distinct red fluorescence. Similar phenomenon is observed when Hg^{2+} ions are used instead, *i.e.*, fluorescence is recovered or depressed in the absence or presence of Hg^{2+} ions (Fig. 4c and d). These results demonstrate successful modification of GA molecules on SiNW surface, and also suggest that our sensing strategy is suitable for facile "naked-eye" detection of DNA or Hg^{2+} with relatively high concentrations (~1 μM) *via* observation of fluorescence "off" and "on".

As in above discussion, fluorescence intensity of Cy5 can be largely recovered in the presence of target DNA whose sequences are listed in Table S1.† As a result, based on monitoring changes of fluorescent intensities, target DNA with serial concentrations can be sensitively detected in our experiment. Fig. 5a–c shows gradual enhancement of fluorescent intensities induced by increase of DNA concentrations. Typically, the fluorescence intensity is ~2589 for target DNA of 1 nM, and gradually reduced to ~2210, ~1742, and ~1449, as the DNA concentration decreases to 100, 10, and 1 pM, respectively. While the intensity is finally reduced to ~1449 at 1 pM target DNA, the value is distinctly larger than that of background (~1127) or non-complementary DNA (~1083). Significantly, the fluorescence changes differ ~80% for wide-ranging concentrations from 1 pM (~1449) to 1 nM (~2589). Such distinct difference is acceptable and comparable to those reported in previous publications.[22,44,53–58] It is worth pointing out that, in case of 10 nM target DNA, their fluorescent intensity (~2690) is similar to that of 1 nM target DNA (~2589), suggesting that the maximum concentration of stem-loop DNA modified on SiNWs (76.09 μg mL^{-1}) surface in 100 μL ranges from 1 to 10 nM, which coincides well with theoretical results (see calculation details in the Experiment section). The SiNWs-based sensor is suitable for discrimination of single-base mismatch. As shown in Fig. 5d and e, the fluorescence intensity is dramatically decreased to ~72% compared to that of complementary DNA-treated group.

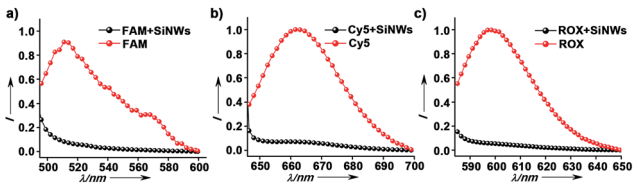

Fig. 3 Fluorescence spectra of SiNWs (85 μg mL^{-1})-treated organic dyes. Typically, compared to strong fluorescence of pure organic dyes (red lines), SiNWs lead to severe fluorescence quenching (black lines) with high QE values towards FAM (91.2%), Cy5 (92.8%), and ROX (94.4%), respectively.

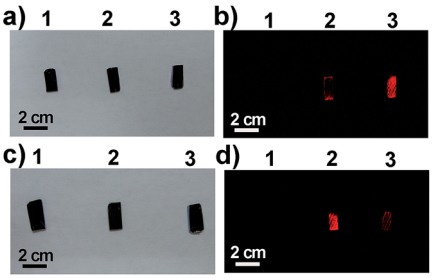

Fig. 4 Images of SiNW arrays on silicon wafers irradiated by ambient light (a and c) or UV light (b and d). (a) and (b) are for DNA detection: (1) control (pure SiNW arrays), (2) stem-loop DNA modified SiNW arrays, (3) loop-structured capture DNA modified SiNW arrays hybridized with target DNA (1 μM). (c) and (d) are for Hg^{2+} detection: (1) control (pure SiNW arrays), (2) T-rich mercury-specific oligonucleotides (MSO)-modified SiNW arrays, (3) T-rich mercury-specific oligonucleotides (MSO)-modified SiNW arrays reacted with Hg^{2+} (1 μM). Note that negligible fluorescence observed in (b-2) and (d-3) is possibly due to non-specific DNA absorption and non-uniform growth of SiNW arrays on silicon wafers. ($\lambda_{excitation}$ = 635 nm; windows: 650–720 nm; exposure time: 150 ms). Scale bars stand for 2 cm.

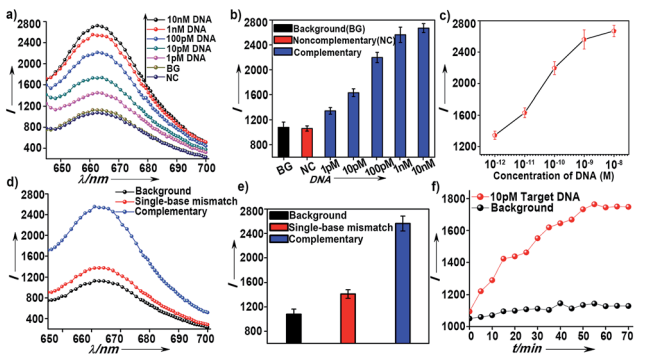

Fig. 5 (a) Fluorescence spectra and (b) corresponding PL intensities of complementary target DNA with serial concentrations. (c) The calibration curve for the fluorescence intensity of SiNWs-based sensors for DNA analysis in the presence of complementary target DNA with serial concentrations. (d) PL spectra and (e) corresponding PL intensities of SiNWs-based sensor with or without treatment of complementary DNA (10 nM) and single-based mismatches ($\lambda_{excitation}$ = 480 nm). (f) Kinetic property of SiNWs-based fluorescent sensors. Error bars indicate standard deviation determined from three repetitions.

As shown in Fig. 5f, kinetic property of the SiNWs-based fluorescent sensor is also investigated. Typically, the sensor maintains stable and feeble fluorescence without target DNA (black line). In contrast, in the presence of target DNA, fluorescent intensity gradually increases accompanied with increase in time, and is fully recovered at ~60 min (red line).

Simultaneous multiplexed detection is of essential importance for practical detection assay. Large surface-to-volume ratio of SiNWs enables simultaneous assembly of multiple DNA strands onto surface of one single SiNW, facilitating construction of high-performance SiNW-based multiplexed sensors. In our experiment (Fig. 6a), SiNWs are simultaneously modified with three types of Cy5, ROX, or FAM-tagged capture DNA, which are ready for multiplexed assay of three classes of tumor-suppressor genes, *i.e.*, exon segments of p16, p21, and p53 genes (see their sequence in Table S2†). As shown in Fig. 6b–d, the sensor produces weak fluorescent signals without target DNA. In marked contrast, once hybridizing with targeted genes, the fluorescence at the maximum emission wavelengths of 516 nm (blue line in Fig. 6b), 666 nm (blue line in Fig. 6c), and 605 nm (blue line in Fig. 6d) are significantly enhanced in case of p16, p21, and p53, respectively.[16,35] For discrimination of single-based mismatches, fluorescence relatively increases, which is up to 24.5% (p16), 30% (p21), or 29% (p53), respectively (red lines in Fig. 6b–d). The above data demonstrate that the resultant SiNWs-based fluorescent sensors are efficacious for multiplexed detection of genes. A consensus has been reached that, for multiplexing detection, the detection limits of the individual cases are dominantly influenced by the different QE values of various organic dyes in multiplex detection, as well as the signal-to-noise ratio of sensing devices.[21,44,59] Notably, taking advantage of high quenching efficiency (QE values > 90%) toward different classes of organic dyes (*e.g.*, FAM, Cy5, and ROX), the SiNWs-based sensors feature a low detection limit of ~10 pM for the multiplexing DNA detection. Fig. 7 shows that the fluorescence of the SiNWs-based fluorescent sensors is gradually enhanced as the target concentration increases from 10 pM to 10 nM.

In addition to sensitive DNA detection, our SiNWs-based sensor modified with specific nucleic acid structures (*e.g.*, aptamers) is also efficacious for detecting heavy metal ions. As a proof of concept, we employ a T-rich mercury-specific oligonucleotide (MSO) tagged with Cy5 molecules for modification of the SiNWs-based sensor, enabling sensitive and specific detection of Hg^{2+} ions.[60–62] In particular, in the absence of Hg^{2+} ions, the MSO-modified SiNW yields strong fluorescence due to relatively long distance between Cy5 molecules and the SiNW (Step 4′ in Fig. 1 and black line in Fig. 8a). In contrast, the loop structure is formed *via* the introduction of Hg^{2+} attributed to specific binding of Hg^{2+} ions to thymine–thymine (T–T) base pairs in DNA duplexes.[60–64] As a result, Cy5 molecules efficiently separate from the SiNW surface, and severe fluorescence quenching is observed due to high quenching efficiency of the SiNW (Step 5′ in Fig. 1). In our experiment, the MSO-modified SiNWs are treated with Hg^{2+} ions of various concentrations (5 pM–5 nM), and the kinetics of the fluorescence decrease at ~666 nm is monitored. As shown in Fig. 8a and b, Hg^{2+} ions of higher concentrations result in more severe fluorescence quenching. Typically, the fluorescence intensity drops approximately to 87%, 78%, 69%, 58%, 51%, or 43% of the original intensity when the DNA concentration gradually increases to 5, 10, 50, 500, 1000, or 5000 pM, respectively. Notably, the intensity of 5 pM Hg^{2+} (~4360) is obviously lower than the control value (~4990), suggesting a low detection limit of Hg^{2+} ions (5 pM) using our sensing strategy. We further determine the selectivity of the sensor through specific detection of Hg^{2+} ions in a mixture solution containing other kinds of interfering metal ions (*i.e.*, Ca^{2+}, Mn^{2+}, Ni^{2+}, Cd^{2+}, Fe^{2+}, Ag^{+}, Cu^{2+}, Zn^{2+}, Mg^{2+}, Co^{2+}, and Ba^{2+}), which are shown in Fig. 8c. Significantly,

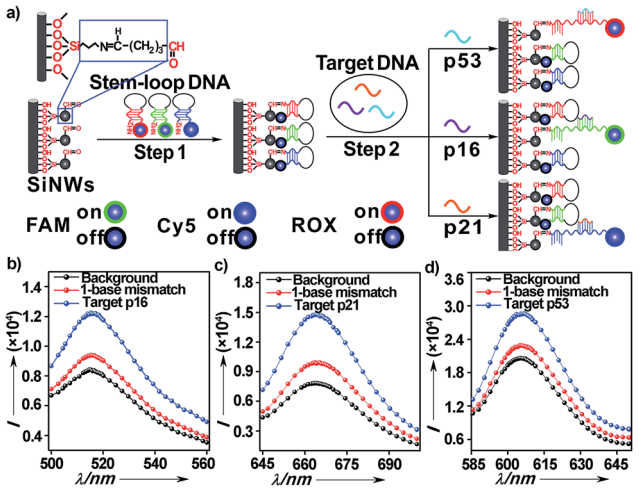

Fig. 6 (a) Schematic illustration of SiNWs-based sensors for multiplexed DNA detection. (b–d) PL spectra of the SiNWs-based sensors in the presence of target DNA (10 nM) or single-based mismatches. For different genes tagged with FAM (p16), Cy5 (p21), and ROX (p53), the maximum emission wavelength is 516 nm ($\lambda_{excitation}$ = 480 nm), 666 nm ($\lambda_{excitation}$ = 643 nm), and 605 nm ($\lambda_{excitation}$ = 578 nm), respectively.

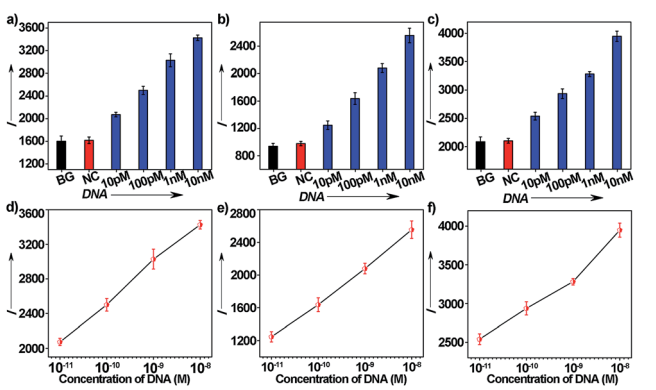

Fig. 7 (a–c) Corresponding fluorescent intensities of SiNWs-based sensors for DNA multiplexed analysis in the presence of complementary target DNA with various concentrations: (a) FAM-tagged probes, (b) Cy5-tagged probes, (c) ROX-tagged probes. (d–f) The calibration curve for the fluorescence intensity of SiNWs-based sensors for multiplexed DNA detection: (d) FAM-tagged probes, (e) Cy5-tagged probes, (f) ROX-tagged probes.

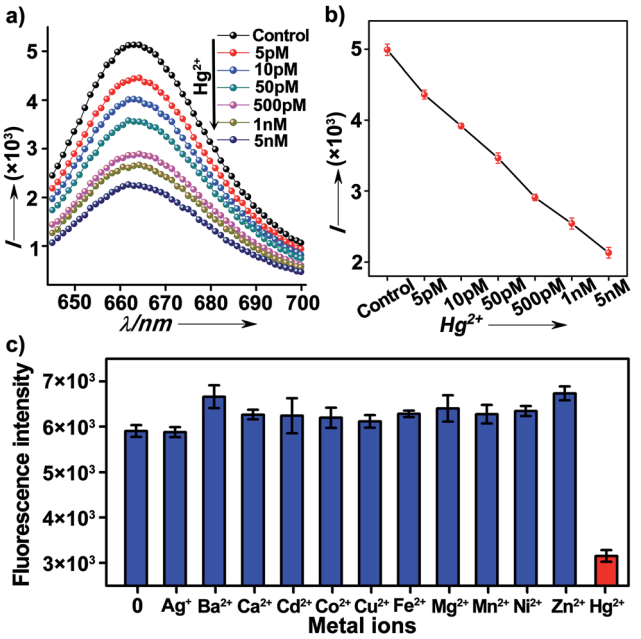

Fig. 8 (a) Fluorescence spectra and (b) corresponding calibration curve of SiNWs-based sensors for detection of Hg^{2+} with serial concentrations. (c) Fluorescence intensity of the SiNWs-based sensor in the presence of various interfering metal ions.

only Hg^{2+} results in distinct decrease of fluorescence signal, which is due to highly specific binding of a T–T pair with Hg^{2+} ions.[60–64]

The SiNWs-based fluorescent sensors are suitable for practical applications, allowing sensitive and specific detection of Hg^{2+} ions in river water obtained from the Dushu Lake, Suzhou, Jiangsu Province, China. The lake water samples are filtered through a 0.22 μm membrane, followed by addition of Hg^{2+} ions of various concentrations (5 pM–5 nM). Fig. 9a presents the calibration curve based on observing changes in fluorescence intensity induced by Hg^{2+} ions (red line). A control DNA (without T–T pairs) is employed as a control, showing relatively stable fluorescence in the presence of Hg^{2+} ions with concentrations ranging from 5 pM to 5 nM (black line). We further interrogate the kinetic property of the SiNWs-based sensor by monitoring the fluorescence decrease at ~666 nm, as shown in Fig. 9b. Typically, in case of Hg^{2+} ions-treated sample, the fluorescent intensity gradually decreases accompanied with reaction time prolonging from 1 to 30 min (red line). In marked contrast, the fluorescence remains constant in the absence of Hg^{2+} ions (black line). Furthermore, other metal ions (*e.g.*, Ca^{2+}, Mn^{2+}, Ni^{2+}, Cd^{2+}, Fe^{2+}, Ag^{+}, Cu^{2+}, Zn^{2+}, Mg^{2+}, Co^{2+}, and Ba^{2+}) are added into the water sample, leading to a negligible change in fluorescence intensities (Fig. 9c), confirming the high specificity of the SiNWs-based sensor.

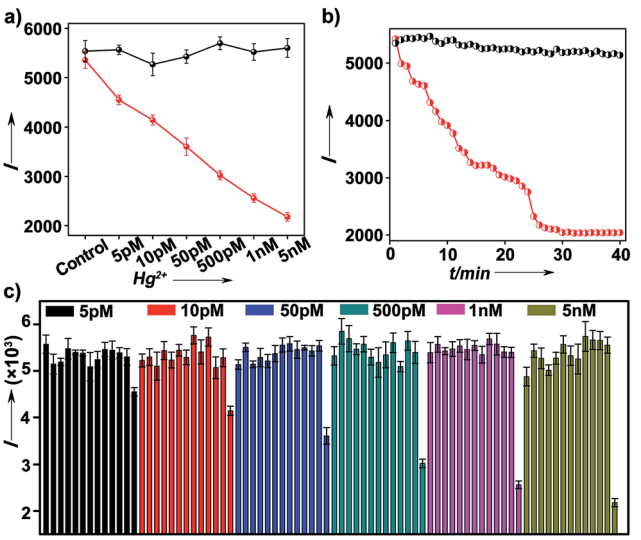

Fig. 9 (a) The calibration curve for the fluorescent intensity of MSO probes (red line) and a control DNA (without T–T pairs) (black line) in the presence of Hg^{2+} of serial concentrations in the real water sample. (b) Kinetic property of MSO probes. (c) Fluorescence intensity of the SiNWs-based sensor in the present of interfering metal ions with different concentrations in the real water (from left to right: control, Ag^{+}, Ba^{2+}, Ca^{2+}, Cd^{2+}, Co^{2+}, Cu^{2+}, Fe^{2+}, Mg^{2+}, Mn^{2+}, Ni^{2+}, Zn^{2+}, and Hg^{2+}).

Experimental

Chemicals and reagents

DNA strands were purchased from TaKaRa Biotechnology (Dalian) Co., Ltd (China) (Tables S1 and S2† show the sequences of DNA). Hydrofluoric acid (HF ≥ 40%), silver nitrate ($AgNO_3$ ≥ 99.8%), nitric acid (HNO_3 65%–68%), and hydrogen peroxide (H_2O_2 ≥ 30%) were purchased from Sinopharm Chemical Reagent Co., Ltd (Shanghai, China). Glutaraldehyde (GA) (≥50%) was purchased from Tokyo Chemical Industry Co., Ltd. 3-Aminoprophyltriethoxysilane (APTES) (≥99%) was purchased from Sigma-Aldrich. Phosphate-doped silicon (100) wafers with a sensitivity of 0.01–0.02 Ω were obtained from Heifei Kejing Materials Technology Co., Ltd (China). Milli-Q water (Millipore) was employed for preparing the solutions.

Instrumentation

UV-vis-near-infrared spectrophotometer (Perkin-Elmer Lambda 750) and spectrofluorometer (HORIBA JOBIN YVON FLUOROMAX-4) were used for measurement of UV-PL spectra. An electron microscope (Philips CM 200) and scanning electron microscope (FEI Quanta 200F) were utilized for TEM/HRTEM and SEM characterizations.

Synthesis and functionalization of SiNWs

Basically, our previously reported HF-assisted etching strategy was used for synthesizing silicon nanowires (SiNWs).[41–44] Typically, acetone, Milli-Q water, and H_2SO_4 (98%) + H_2O_2 (30%) mixture solution (volume ration: 3 : 1) were sequentially employed for washing the silicon wafer. The cleaned Si wafer was then treated by HF (5%) for 30 min to produce the H-terminated Si wafer. Afterwards, the resultant sample was immediately immersed in the silver nitrate ($AgNO_3$) and HF (10%) mixture solution with slow stirring for 3 min, and finally treated with the HF (10%) and H_2O_2 (0.4 M) for 5 min,

producing the SiNW (diameter: 100–200 nm, length: ~4 μm) arrays on surface of Si wafer (Fig. 2).

For functionalization of SiNWs, the as-prepared SiNW arrays were firstly treated with O_2 plasma for 3 min at 300 W and 200 SCCM (SCCM denotes cubic centimeter per minute at STP) flow rate (Step 1 in Fig. 1), followed by conjugation with 1% (v/v) APTES in pure ethanol for about 2 h at room temperature (Step 2 in Fig. 1), and then reaction with 2.5% (v/v) GA for about 1 h at room temperature (Step 3 in Fig. 1), yielding the GA-modified SiNWs.[45,65–67] Ultrasonic treatment was employed for detaching the resultant GA-modified SiNWs from silicon wafer, which were collected for fabricating the SiNWs-based fluorescent sensors.

SiNWs-based sensors for DNA detection

Briefly, 1 μL of the loop-structured capture DNA (10 μM) was dropped into 100 μL of buffer solution (10 mM Tris–HCl, pH 8.0, 100 mM KCl, 1 mM $MgCl_2$) dispersed with 7.609 μg GA-modified SiNWs. The resultant mixture was kept in a sealed box for 12 h. During this period, the GA-modified SiNWs are readily assembled with the capture DNA that were tagged with amino group and organic dye molecule (*e.g.*, Cy5) at 3 and 5, respectively, by the Schiff reaction, which produced the stem-loop DNA-modified SiNWs. The as-prepared capture DNA-modified SiNWs were further purified through repetitive centrifugation (12 000 rpm, 15 min, 4 °C) and washed there time with PBS buffer (100 mM, pH 7.0). The clean product served as SiNWs-based fluorescent sensors for DNA detection. In our experiment, 1 μL of the target DNA strands was hybridized with the stem-loop capture DNA strands modified on the SiNWs surface in 100 μL hybridization buffer (pH 8.0, 100 mM KCl, 1 mM $MgCl_2$, 10 mM Tris–HCl) for 30 min at 37 °C, and then for 2 h at 25 °C. The hybridization resulted in disruption of stem-loop configuration, leading to enhancement of fluorescence, which could be readily detected by the spectrofluorometer. In our experiment, serial concentrations (1 pM–10 nM) of target DNA were sensitively detected by using the above strategy. In terms of detection of single-based mismatches, the procedures were the same as the above-mentioned routines.

SiNWs-based sensors for multiplexed detection of tumor-suppressor genes

Three classes of organic dyes, *i.e.*, carboxyfluorescein (FAM), cyanine 5 (Cy5), and 6-carboxy-X-rhodamine (ROX)-tagged stem-loop DNA, whose sequences are specifically hybridized with exon segments of p16, p21, and p53 genes, respectively, were simultaneously modified on the surface of GA-modified SiNWs to yield the SiNWs-based sensors with multiplexed sensing capabilities. The resultant sensors were ready for multiplexed detection of p16, p21, and p53 genes. Briefly, three kinds of fluorophores, *i.e.*, FAM-, Cy5-, and ROX-tagged stem-loop DNA (1 μL, 10 μM), were simultaneously dropped into 100 μL of buffer (10 mM Tris–HCl, pH 8.0, 100 mM KCl, 1 mM $MgCl_2$) dispersed with 7.609 μg GA-modified SiNWs. The resultant mixture was kept in a sealed box for 12 h. As a result, the GA-modified SiNW was readily assembled with the three types of capture DNA that were tagged with amino group and organic dye molecule (*i.e.*, FAM, Cy5, and ROX) at 3 and 5, respectively, by the Schiff reaction, which produced the multiple capture DNA-modified SiNWs sensor for multiplexed detection of p16, p21, and p53 genes.[16,21,44] Typically, 1 μL of p16, p21, or p53 genes were hybridized with the stem-loop capture DNA strands modified on the SiNWs surface in 100 μL hybridization buffer (pH 8.0, 100 mM KCl, 1 mM $MgCl_2$, 10 mM Tris–HCl) for 30 min at 37 °C, and then for 2 h at 25 °C. Based on similar "signal-on" principle, fluorescence recovery was sensitively detected using the spectrofluorometer. As a result, p16, p21, and p53 genes with concentrations ranging from 10 pM to 10 nM were readily detected in our experiment. For the detection of single-based mismatches, the procedures were the same as the above-mentioned manipulations.

The loading of the SiNWs with the stem-loop nucleic acid probes was calculated based on a well-studied method.[68] In particular, the modified SiNWs were fully hybridized with the fluorophore-tagged loop-structured DNA (1×10^{-2} nmol) in 100 μL of buffer, containing SiNWs at a concentration of 76.09 μg mL^{-1} in a sealed box overnight. Afterwards, centrifugation was employed for precipitation of the DNA-modified SiNWs (12 000 rpm, 15 min, and 4 °C). Residual DNA featuring an optical density of 0.003114 at 260 nm in the supernatant was then calculated as 0.89×10^{-2} nmol by a previously reported method.[68] As a result, we deduced that stem-loop DNA strands with a saturation concentration of 11 nM were loaded on the SiNWs, consistent with our experimental results (*i.e.*, fluorescent intensity reached the maximum value in the presence of 1–10 nM target DNA).

SiNWs-based sensors for Hg^{2+} detection

1 μL of Cy5-modified mercury specific oligonucleotide (1 μM), a kind of aptamer with the affinity constant of 1.4×10^6 M^{-1},[69] was dropped into 100 μL of buffer solution (10 mM Tris–HCl, 50 mM $NaNO_3$, pH 7.2) dispersed with GA-modified SiNWs (85 μg mL^{-1}). The resultant mixture solution was kept in a sealed box for 12 h. During this period, the GA-modified SiNWs are readily assembled with the capture DNA that were tagged with amino group and organic dye molecule (*e.g.*, Cy5) at 3 and 5, respectively, by the Schiff reaction, which produced the mercury specific oligonucleotide-modified SiNWs ready for detection of Hg^{2+} ions. In our experiment, 1 μL of the Hg^{2+} ions solution was dropped into the above-mentioned solution, and then kept in a sealed box for 3 h at 25 °C. The added Hg^{2+} ions resulted in formation of stem-loop configuration, leading to decrease of fluorescence, which could be readily detected by the spectrofluorometer. In our experiment, serial concentrations (5 pM–5 nM) of Hg^{2+} ions were sensitively detected by using the above strategy. To verify specificity of the SiNWs-based sensors, 100 nM interfering metal ions (*i.e.*, Ca^{2+}, Mn^{2+}, Ni^{2+}, Cd^{2+}, Fe^{2+}, Ag^{+}, Cu^{2+}, Zn^{2+}, Mg^{2+}, Co^{2+}, and Ba^{2+}) were used instead of Hg^{2+} ions. Other manipulations were identical to the above-mentioned procedures.

For detection in real water sample, the real water sample was obtained from the Dushu Lake, Suzhou, Jiangsu Province,

China. The sample was filtered through a 0.22 μm membrane, followed by addition of Hg^{2+} ions of various concentrations (5 pM–5 nM). All the manipulations are identical to the above-mentioned procedures. To verify specificity of the SiNWs-based sensors, interfering metal ions (*i.e.*, Ca^{2+}, Mn^{2+}, Ni^{2+}, Cd^{2+}, Fe^{2+}, Ag^{+}, Cu^{2+}, Zn^{2+}, Mg^{2+}, Co^{2+}, and Ba^{2+}) with various concentrations ranging from 5 pM to 5 nM were used instead of Hg^{2+} ions. Other manipulations were identical to the above-mentioned procedures.

Conclusions

We herein present a kind of high-performance SiNWs-based fluorescent biochemical sensor to take advantage of the unique merits of SiNWs. Of particular significance, the sensor is highly efficacious for multiplexed detection of DNA targets at ~pM levels. In addition to DNA detection, the sensor is capable of detecting metal ions based on the similar signal-on-off principle, allowing sensitive and specific detection of 5 pM Hg^{2+} ions in real water samples. These results suggest this signal-on-off sensing strategy affords high-efficacy means for sensitive and specific detection of wide-ranging chemical and biological analysis. Given SiNWs can be fabricated in reproducible and low-cost manners,[38–44] we believe that the novel SiNWs-based sensors are highly practical for wide-ranging biochemical analysis and detection.

Acknowledgements

The authors appreciate the financial support from the National Basic Research Program of China (973 Program 2013CB934400 and 2012CB932400), the Funds for International Cooperation and Exchange of the National Natural Science Foundation of China (Grant no. 61361160412), the Natural Science Foundation of Jiangsu Province of China (Grant no. BK20130052 and BK20130298), and the Six Talent Peaks Project of Jiangsu Province (Grant no. 2013-XCL-036).

Notes and references

1 H. Craighead, *Nature*, 2006, **442**, 387.
2 P. W. Barone, R. S. Parker and M. S. Strano, *Anal. Chem.*, 2005, **77**, 7556.
3 S. J. Son, J. Reichel, B. He, M. Schuchman and S. B. Lee, *J. Am. Chem. Soc.*, 2005, **127**, 7316.
4 Y. Cui, Q. Q. Wei, H. K. Park and C. M. Lieber, *Science*, 2001, **293**, 1289.
5 F. Patolsky, G. F. Zheng and C. M. Lieber, *Nat. Protoc.*, 2006, **1**, 1711.
6 P. Alivisatos, *Nat. Biotechnol.*, 2004, **22**, 47.
7 X. H. Gao, Y. Y. Cui, R. M. Levenson, L. W. K. Chung and S. M. Nie, *Nat. Biotechnol.*, 2004, **22**, 969.
8 X. Michalet, F. F. Pinaud, L. A. Bentolila, J. M. Tsay, S. Doose, J. J. Li, G. Sundaresan, A. M. Wu, S. S. Gambhir and S. Weiss, *Science*, 2005, **307**, 538.
9 R. Freeman and I. Willner, *Chem. Soc. Rev.*, 2012, **41**, 4067.
10 Y. C. Cao, R. C. Jin and C. A. Mirkin, *Science*, 2002, **297**, 1536.
11 H. H. Wang, C. Y. Liu, S. B. Wu, N. W. Liu, C. Y. Peng, T. H. Chan, C. F. Hsu, J. K. Wang and Y. L. Wang, *Adv. Mater.*, 2006, **18**, 491.
12 D. Graham, D. G. Thompson, W. E. Smith and K. Faulds, *Nat. Nanotechnol.*, 2008, **3**, 548.
13 S. R. Dasary, A. K. Singh, D. Senapati, H. Yu and P. C. Ray, *J. Am. Chem. Soc.*, 2009, **131**, 13806.
14 K. L. Wustholz, A. L. Henry, J. M. McMahon, R. G. Freeman, N. Valley, M. E. Piotti, M. J. Natan, G. C. Schatz and R. P. V. Duyne, *J. Am. Chem. Soc.*, 2010, **132**, 10903.
15 E. Sharon, R. Freeman, M. Riskin, N. Gil, Y. Tzfati and I. Willner, *Anal. Chem.*, 2010, **82**, 8390.
16 S. P. Song, Z. Q. Zhang, J. Zhang, L. H. Wang, G. X. Li and C. H. Fan, *Angew. Chem., Int. Ed.*, 2009, **48**, 8670.
17 S. P. Song, Y. Qin, Y. He, Q. Huang and C. H. Fan, *Chem. Soc. Rev.*, 2010, **39**, 4234.
18 D. J. Maxwell, J. R. Taylor and S. M. Nie, *J. Am. Chem. Soc.*, 2002, **124**, 9606.
19 C. H. Lu, H. H. Yang, C. L. Zhu, X. Chen and G. N. Chen, *Angew. Chem., Int. Ed.*, 2009, **121**, 4879.
20 R. H. Yang, J. Y. Jin, Y. Chen, N. Shao, H. Z. Kang, Z. Y. Xiao, Z. W. Tang, Y. R. Wu, Z. Zhu and W. H. Tan, *J. Am. Chem. Soc.*, 2008, **130**, 8351.
21 S. J. He, B. Song, D. Li, C. F. Zhu, W. P. Qi, Y. Q. Wen, L. H. Wang, S. P. Song, H. P. Fang and C. H. Fan, *Adv. Funct. Mater.*, 2010, **20**, 453.
22 S. Shimron, A. Cecconello, C. H. Lu and I. Willner, *Nano Lett.*, 2013, **13**, 3791.
23 L. Pavesi, L. D. Negro, C. Mazzoleni, G. Franzo and F. Priolo, *Nature*, 2000, **408**, 440.
24 Z. F. Ding, B. M. Quinn, S. K. Haram, L. E. Pell, B. A. Korgel and A. J. Bard, *Science*, 2002, **296**, 1293.
25 F. Patolsky, B. P. Timko, G. H. Yu, Y. Fang, A. B. Greytak, G. F. Zheng and C. M. Lieber, *Science*, 2006, **313**, 1100.
26 Y. He, Y. Y. Su, X. B. Yang, Z. H. Kang, T. T. Xu, R. Q. Zhang, C. H. Fan and S. T. Lee, *J. Am. Chem. Soc.*, 2009, **131**, 4434.
27 Y. He, Z. H. Kang, Q. S. Li, C. H. A. Tsang, C. H. Fan and S. T. Lee, *Angew. Chem., Int. Ed.*, 2009, **121**, 134.
28 Y. He, C. H. Fan and S. T. Lee, *Nano Today*, 2010, **5**, 282.
29 D. D. D. Ma, C. S. Lee, F. C. K. Au, S. Y. Tong and S. T. Lee, *Science*, 2003, **299**, 1874.
30 K. Q. Peng and S. T. Lee, *Adv. Mater.*, 2011, **23**, 198.
31 W. Kim, J. K. Ng, M. E. Kunitake, B. R. Conklin and P. D. Yang, *J. Am. Chem. Soc.*, 2007, **129**, 7228.
32 Y. Jung, L. Tong, A. Tanaudommongkon, J. X. Cheng and C. Yang, *Nano Lett.*, 2009, **9**, 2440.
33 Z. Li, J. H. Song, G. Mantini, M. Y. Lu, H. Fang, C. Falconi, L. J. Chen and Z. L. Wang, *Nano Lett.*, 2009, **9**, 3575.
34 M. Lv, S. Su, Y. He, Q. Huang, W. B. Hu, D. Li and C. H. Fan, *Adv. Mater.*, 2010, **22**, 5463.
35 M. W. Shao, L. Cheng, X. H. Zhang, D. D. D. Ma and S. T. Lee, *J. Am. Chem. Soc.*, 2009, **131**, 17738.
36 Y. Q. Qu, L. Liao, Y. J. Li, H. Zhang, Y. Huang and X. F. Duan, *Nano Lett.*, 2009, **9**, 4539.
37 A. I. Hochbaum, D. Gargas, Y. J. Hwang and P. D. Yang, *Nano Lett.*, 2009, **9**, 3550.

38 Y. He, Y. L. Zhong, F. Peng, X. P. Wei, Y. Y. Su, S. Su, W. Gu, L. S. Liao and S. T. Lee, *Angew. Chem., Int. Ed.*, 2011, **123**, 3136.
39 Y. Y. Su, X. P. Wei, F. Peng, Y. L. Zhong, Y. M. Lu, S. Su, T. T. Xu, S. T. Lee and Y. He, *Nano Lett.*, 2012, **12**, 1845.
40 F. Peng, Y. Y. Su, X. P. Wei, Y. M. Lu, Y. F. Zhou, Y. L. Zhong, S. T. Lee and Y. He, *Angew. Chem., Int. Ed.*, 2013, **52**, 1457.
41 Y. He, S. Su, T. T. Xu, Y. L. Zhong, J. A. Zapien, J. Li, C. H. Fan and S. T. Lee, *Nano Today*, 2011, **6**, 122.
42 Y. L. Zhong, F. Peng, X. P. Wei, Y. F. Zhou, J. Wang, X. X. Jiang, Y. Y. Su, S. Su, S. T. Lee and Y. He, *Angew. Chem., Int. Ed.*, 2012, **51**, 8485.
43 Y. He, Y. L. Zhong, F. Peng, X. P. Wei, Y. Y. Su, Y. M. Lu, S. Su, W. Gu, L. S. Liao and S. T. Lee, *J. Am. Chem. Soc.*, 2011, **133**, 14192.
44 S. Su, X. P. Wei, Y. L. Zhong, Y. Y. Guo, Y. Y. Su, Q. Huang, S. T. Lee, C. H. Fan and Y. He, *ACS Nano*, 2012, **6**, 2582.
45 C. C. Wu, F. H. Ko, Y. S. Yang, D. L. Hsia, B. S. Leea and T. S. Su, *Biosens. Bioelectron.*, 2009, **25**, 820.
46 S. T. Kim, D. J. Kim, T. J. Kim, D. W. Seo, T. H. Kim, S. Y. Lee, K. Kim, K. M. Lee and S. K. Lee, *Nano Lett.*, 2010, **10**, 2877.
47 J. L. He, Y. Ba, C. I. Ratcliffe, J. A. Ripmeester, D. D. Klug, J. S. Tse and K. F. Preston, *J. Am. Chem. Soc.*, 1998, **120**, 10697.
48 Y. L. Zhong, F. Peng, F. Bao, S. Y. Wang, X. Y. Ji, Y. Y. Su, S. T. Lee and Y. He, *J. Am. Chem. Soc.*, 2013, **135**, 8350.
49 Y. Kato, H. Yamazaki and M. Tomozawa, *J. Am. Ceram. Soc.*, 2001, **84**, 2111.
50 K. S. Dancil, D. P. Greiner and M. J. Sailor, *J. Am. Chem. Soc.*, 1999, **121**, 7925.
51 M. Zayats, Y. Huang, R. Gill, C. Ma and I. Willner, *J. Am. Chem. Soc.*, 2006, **128**, 13666.
52 B. L. Frey and R. M. Corn, *Anal. Chem.*, 1996, **68**, 3187.
53 D. Li, A. Wieckowska and I. Willner, *Angew. Chem., Int. Ed.*, 2008, **120**, 3991.
54 G. Mor-Piperberg, R. Tel-Vered, J. Elbaz and I. Willner, *J. Am. Chem. Soc.*, 2010, **132**, 6878.
55 S. Liu, J. Q. Tian, L. Wang, Y. W. Zhang, X. Y. Qin, Y. L. Luo, A. M. Asiri, A. O. Al-Youbi and X. P. Sun, *Adv. Mater.*, 2012, **24**, 2037.
56 W. B. Lu, X. Y. Qin, S. Liu, G. H. Chang, Y. W. Zhang, Y. L. Luo, A. M. Asiri, A. O. Al-Youbi and X. P. Sun, *Anal. Chem.*, 2012, **84**, 5351.
57 D. Han, S. Y. Lim, B. J. Kim, L. L. Piao and T. D. Chung, *Chem. Commun.*, 2010, **46**, 5587.
58 W. T. Huang, Y. Shi, W. Y. Xie, H. Q. Luo and N. B. Li, *Chem. Commun.*, 2011, **47**, 7800.
59 D. Horejsh, F. Martini, F. Poccia, G. Ippolito, A. D. Caro and M. R. Capobianchi, *Nucleic Acids Res.*, 2005, **33**, 1.
60 A. Ono and H. Togashi, *Angew. Chem., Int. Ed.*, 2004, **43**, 4300.
61 Z. Q. Zhu, Y. Y. Su, J. Li, D. Li, J. Zhang, S. P. Song, Y. Zhao, G. Li and C. H. Fan, *Anal. Chem.*, 2009, **81**, 7660.
62 B. J. Lee, H. Jun and J. Kim, *Adv. Mater.*, 2009, **21**, 3674.
63 X. F. Liu, Y. L. Tang, L. H. Wang, J. Zhang, S. P. Song, C. H. Fan and S. Wang, *Adv. Mater.*, 2007, **19**, 1471.
64 Y. Miyake, H. Togashi, M. Tashiro, H. Yamaguchi, S. Oda, M. Kudo, Y. Tanaka, Y. Kondo, R. Sawa, T. Fujimoto, T. Machinami and A. Ono, *J. Am. Chem. Soc.*, 2006, **128**, 2172.
65 Y. L. Bunimovich, Y. S. Shin, W. S. Yeo, M. Amori, G. Kwong and J. R. Heath, *J. Am. Chem. Soc.*, 2006, **128**, 16323.
66 Z. Li, Y. Chen, X. Li, T. I. Kamins, K. Nauka and R. S. Williams, *Nano Lett.*, 2004, **4**, 245.
67 G. J. Zhang, J. H. Chua, R. E. Chee, A. Agarwal, S. M. Wong, K. D. Buddharaju and N. Balasubramanian, *Biosens. Bioelectron.*, 2008, **23**, 1701.
68 J. Li, S. P. Song, D. Li, Y. Su, Q. Huang, Y. Zhao and C. H. Fan, *Biosens. Bioelectron.*, 2009, **24**, 3311.
69 Y. Wang, Y. Zheng, F. Yang and X. R. Yang, *Chem. Commun.*, 2012, **48**, 2873.

